that a similar metal–metal structuring can be assumed in all the samples.

The $Q(r)$ of Fe–B–O exhibits sharp peaks up to large r values, thus confirming for this compound a definitely more ordered structure than in the other two, as concluded from the appearance of the diffraction spectrum.

All $Q(r)$'s show a small peak at around 2 Å that is due to metal–metalloid interaction but, as the samples contain both boron and oxygen, a definite assignment cannot be made.

The short- and medium-range order in the as-prepared samples, as inferred by the inspection of pertinent $Q(r)$'s, increases in the sequence Co < Ni < Fe, which is opposite to the reactivity of the cations in the chemical reduction by KBH_4.[15] This suggests that high reaction rates could hinder an ordered structural organization of the products. The amorphous character also seems to be correlated with the boron content of the samples. It is, however, difficult to assess whether this depends only on the boron portion present in the metal bulk, as in the many metal–boron amorphous alloys reported in the literature,[29] or also on the relevant presence of borates; these could in fact play the role of a stabilizing matrix of the materials. The second hypothesis is instead supported in our samples by the low content of boron in the bulk, as shown by the low content or absence of metal borides in the spectra of the heat-treated samples.

Acknowledgment. This work has been supported by Consiglio Nazionale delle Ricerche (CNR Contract No. 88.00150.11).

Registry No. KBH_4, 13762-51-1; Co–B–O, 126543-36-0; Ni–B–O, 126543-37-1; Fe–B–O, 126543-38-2; Co_3B, 12006-78-9; CO_2B, 12045-01-1; Ni_3B, 12007-02-2.

(29) Davies, H. A. In ref 1, p 8.

Pressure Dependence of the Raman Spectra of Quasi-One-Dimensional Mixed-Valence Semiconductors and Related Complexes

Mary Ann Stroud, Scott A. Ekberg, and Basil I. Swanson*

Isotope and Nuclear Chemistry Division, Los Alamos National Laboratory, Los Alamos, New Mexico 87545

Received November 20, 1989

The effects of pressure on the resonance Raman spectra of the mixed-valence semiconductors $K_4[Pt_2(P_2O_5H_2)_4X]\cdot 3H_2O$, X = Cl, Br ($Pt_2X$), have been investigated. The related complexes $K_4[Pt_2(P_2O_5H_2)_4X_2]\cdot 2H_2O$, X = Cl, Br ($Pt_2X_2$), and $[(Bu)_4N]_4[Pt_2(P_2O_5H_2)_4]$ (Pt_2) have also been studied so that direct comparisons with the monohalides could be made. Reduction in the intensity of the Pt–Br and a Pt–Pt stretch in the delocalized form of Pt_2Br provide evidence for a pressure-induced structural change from a distorted ground state toward a symmetric structure in which the halogen is centrally located between adjacent Pt dimers. No significant intensity changes were observed in the trapped valence Pt_2Br or in Pt_2Cl, indicating that these complexes remain strongly trapped valence to 5.0 and 10.0 GPa, respectively. Pt_2Br_2 undergoes a pressure-induced phase transition at approximately 2.0 GPa. No transformation was observed in Pt_2Cl_2 to 7.5 GPa. Pressure effects on Raman modes associated with local defect states in Pt_2Cl, Pt_2Cl_2, and delocalized Pt_2Br are also reported. The frequencies of the defect modes shifted toward those of the analogous bulk mode with increasing pressure, suggesting that the defect states become increasingly delocalized with increasing pressure.

Introduction

Quasi-one-dimensional halide-bridged mixed-valence transition-metal complexes MX and MMX have recently received a great deal of attention as model low-dimensional solids exhibiting valence fluctuations and local gap states.[1-12] These complexes are generally in the strongly trapped valence, charge density wave limit with the halogen distorted from the central position between the metal atoms due to a Peierls instability. A new trapped valence form of $K_4[Pt_2(P_2O_5H_2)_4Br]\cdot 3H_2O$ (TV–Pt_2Br) and $K_4[Pt_2(P_2O_5H_2)_4Cl]\cdot 3H_2O$ (Pt_2Cl) are in this limit. However, an increasing number of mixed-valence solids, particularly the delocalized valence form of $K_4[Pt_2(P_2O_5H_2)_4Br]\cdot 3H_2O$ (DV–Pt_2Br), have been found to be much more valence delocalized with small distortion of the halide sublattice.[13-15] A Ni^{III}–X–Ni^{III} complex with no distortion of the halide has recently been synthesized.[16] An emerging

(1) Ueta, M.; Kanzaki, H.; Kobayashi, K.; Toyazawa, Y.; Hanamura, E. *Excitonic Processes in Solids*; Springer Series in Solid State Sciences: Berlin, 1986; Vol. 60, Chapter 9.
(2) Keller, H. J. *Extended Linear Chain Compounds*; Miller, J. S., Ed.; Plenum: New York, 1982; pp 357.
(3) Clark, R. J. H. *Advances in Infrared and Raman Spectroscopy*; Vol. 11, Clark, R. J. H., Hester, R. E., Ed.; Wiley: Heyden, 1984; p 95.
(4) Clark, R. J. H. *Mixed Valence Compounds*; Brown, D. B., Ed.; Reidel: Dordrecht, 1982; p 271.
(5) Clark, R. J. H.; Kurmoo, M. *J. Chem. Soc., Faraday Trans.* **1983**, *79*, 519.
(6) Tanaka, M.; Kurita, S.; Kojima, T.; Yamada, Y. *Chem. Phys.* **1984**, *91*, 257.
(7) Tanaka, M.; Kurita, S. *J. Phys. C: Solid State Phys.* **1986**, *19*, 3019.
(8) Conradson, S. D.; Dallinger, R. F.; Swanson, B. I.; Clark, R. J. H.; Croud, V. B. *Chem. Phys. Lett.* **1987**, *135*, 463.
(9) Conradson, S. D.; Stroud, M. A.; Zietlow, M. H.; Swanson, B. I. *Solid State Commun.* **1988**, *65*, 723.
(10) Onodera, Y. *Phys. Soc. Jpn.* **1987**, *56*, 250.
(11) Baeriswyl, D.; Bishop, A. R. *J. Phys. C: Solid State Phys.* **1988**, *21*, 339.
(12) Baeriswyl, D.; Bishop, A. R. *Phys. Scr.*, in press.
(13) Kurmoo, M.; Clark, R. J. H. *Inorg. Chem.* **1985**, *24*, 4420.
(14) Che, C.-M.; Herbstein, F. H.; Schaefer, W. P.; Marsh, R. E.; Gray, H. B. *J. Am. Chem. Soc.* **1983**, *105*, 4604.
(15) Butler, L. G.; Zietlow, M. H.; Che, C.-M.; Schaefer, W. P.; Sridhar, S.; Grunthaner, P. J.; Swanson, B. I.; Clark, R. J. H.; Gray, H. B. *J. Am. Chem. Soc.* **1988**, *110*, 1155.
(16) Toriumi, K.; Wada, Y.; Mitani, T.; Bandow, S. *J. Am. Chem. Soc.* **1989**, *111*, 2341.

0897-4756/90/2802-0366$02.50/0

Table I. Assignments and Ambient-Pressure Frequencies (cm^{-1}) of Raman Modes

	Pt_2Cl_2	Pt_2Cl	Pt_2Br_2	TV-Pt_2-Br	DV-Pt_2-Br	Pt_2
Pt^{II}–Pt^{II} defect		119		120	116	116
	116, 121	125				
Pt^{III}–Pt^{III} defect	159	157	129	136	121	
		154			134	
unassigned ring-bending mode	201				201	
		262				
Pt–X defect	308	302	216	222	211	
		293			222	

characteristic of these materials is that their physical properties may be tuned by varying the transition-metal complex ions, the halogen, and external pressure.[17-24]

A study of the effects of high pressure on the resonance Raman spectra of the Pt_2X complexes, obtained by excitation into the intervalance charge-transfer (IVCT) band, was undertaken to determine the structural and chemical changes that occur with increasing hydrostatic pressure. The effects of pressure on the Raman spectra of the related complexes $K_4[Pt_2(P_2O_5H_2)_4X_2]\cdot 2H_2O$, X = Cl, Br ($Pt_2X_2$), and $[(Bu)_4N]_4[Pt_2(P_2O_5H_2)_4]$ (Pt_2) have also been investigated so that direct comparison with the monohalides could be made.[25] The structure of the metal axis of $K_4[Pt_2(P_2O_5H_2)_4]\cdot 2H_2O$, Pt_2X, and Pt_2X_2 complexes are illustrated as follows:

$$\begin{array}{c} Pt^{II}—Pt^{II} \\ -X—Pt^{II+\delta}—Pt^{II+\delta}—X—Pt^{III-\delta}—Pt^{III-\delta}—X- \\ X—Pt^{III}—Pt^{III}—X \\ 0 < \delta < 0.5 \end{array}$$

Binuclear platinum diphosphite solids exhibit a number of different defect states resulting from slight stoichiometric imbalances. The effects of pressure on defect states in Pt_2Cl_2 and DV-Pt_2Br, as well as the Pt_2Cl polaron, are also reported.

Experimental Apparatus and Procedures

Pressure was generated with use of a gasketed Merrill-Basset diamond anvil cell. Low-temperature data were obtained by coupling the diamond anvil cell to the cold end of an Air Products displex closed-cycle refrigeration system. Reported temperatures were determined with use of a thermocouple attached to the cell. In the low-temperature experiments, the cell was warmed to at least 120 K before the pressure was increased to allow for proper equilibration and to reduce strain on the cell. Ruby fluorescence pressure calibration method was used to determine pressures.[26]

Raman spectra and fluorescence measurements were obtained on a SPEX Model 1403 $^3/_4$-m double monochromator equipped with a Princeton Applied Research photon-counting system using a backscattering technique. Spectra-Physics 171 argon and krypton lasers were used as a light source. Because of problems with sample degradation, laser power at the sample was kept to 3–20 mW, depending on the complex.

The complexes were prepared by published procedures.[13-15,27,28] Data were generally collected on a sample of several small crystals; however, the Pt_2Cl polaron data were obtained on ground samples. Mineral oil was employed as the pressurizing medium for Pt_2Cl_2 and Pt_2Br_2, and hexane was used for Pt_2, Pt_2Cl, and both forms of Pt_2Br. Mineral oil was not used in the low-temperature experiments because anisotropic conditions were observed with mineral oil at low temperatures and pressures. At least two pressure runs were conducted on each material to ensure reproducibility.

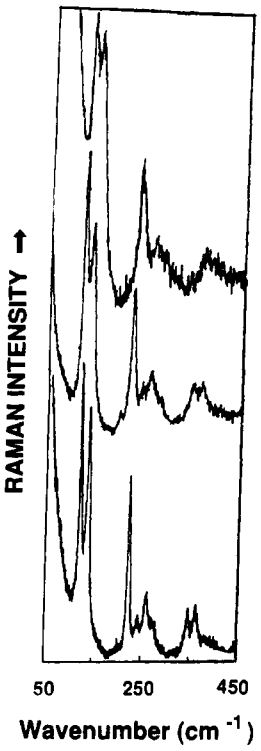

Figure 1. Raman spectra of TV-Pt_2Br obtained at several pressures by using 647.1-nm excitation.

Results

Assignments and ambient pressure wavenumbers of pertinent Raman modes in all complexes studied are summarized in Table I.

Pt_2X. The pressure dependence of the Raman spectra of TV-Pt_2Br at 20 K obtained by using 647.1-nm excitation is shown in Figure 1. No significant intensity changes were observed in TV-Pt_2Br to 5.0 GPa. The pressure-induced effects were reversible when considerable care was taken to ensure conditions were hydrostatic. *Nonhydrostatic compression resulted in an irreversible conversion of*

(17) Interrante, L. V.; Browall, K. W.; Bundy, F. P. *Inorg. Chem.* **1974**, *13*, 1158.
(18) Tanino, H.; Koshizuka, N.; Hoh, K.; Kato, K.; Yamashita, M.; Kobayashi, K. *Physica* **1986**, *39*, 140B, 487.
(19) Tanino, H.; Koshizuka, N.; Kobayashi, K.; Yamashita, M. *Solid State Physics under Pressure*; Minomura, S., Ed.; Terra Scientific: 1985; p 115.
(20) Tanino, H.; Koshizuka, N.; Kobayashi, K.; Yamashita, M.; Hoh, K. *J. Phys. Soc. Jpn.* **1985**, *54*, 483.
(21) Stroud, M. A.; Drickamer, H. G.; Zietlow, M. H.; Gray, H. B.; Swanson, B. I. *J. Am. Chem. Soc.* **1989**, *111*, 66.
(22) Swanson, B. I.; Stroud, M. A.; Conradson, S. D.; Zietlow, M. H. *Solid State Commun.* **1988**, *65*, 1405.
(23) Whangbo, M.-H.; Foshee, M. J. *Inorg. Chem.* **1981**, *20*, 113.
(24) Whangbo, M.-H.; Canadell, E. *Inorg. Chem.* **1986**, *25*, 1726.
(25) Pt_2, Pt_2X_2, and Pt_2X consist of two square-planar Pt units held together by four bidentate pyrrophosphite ligands; $[(HO_2P)_2O^{2-}]Pt_2Cl_2$ has a triclinic cell with a $P\bar{1}$ space group. In $K_4[Pt_2(P_2O_5H_2)_4\cdot 2H_2O$, Pt_2Br_2, Pt_2Cl, and Pt_2Br the metal–metal bond is aligned along the z axis of the tetragonal unit cell. $K_4[Pt_2(Pt_2O_5H_2)_4\cdot 2H_2O$, PtCl, and trapped valence Pt_2Br have a $P4/mbm$ space group and Pt_2Br_2 is $I4/mmm$. For the monohalides the units repeat, forming an infinite linear chain in the z direction. The crystal structure of delocalized Pt_2Br and Pt_2 have not been reported.
(26) The cell was allowed to equilibrate after each pressure increase, and ruby fluorescence was routinely checked before and after the data collection. When possible, the fluorescence from several rubies located in different parts of the cell were measured.
(27) Che, C.-M.; Schaefer, W. P.; Gray, H. B.; Dickson, M. K.; Stein, P. B.; Roundhill, D. M. *J. Am. Chem. Soc.* **1982**, *104*, 4253.
(28) Che, C.-M.; Butler, L. G.; Grunthaner, P. J.; Gray, H. B. *Inorg. Chem.* **1985**, *24*, 4662.

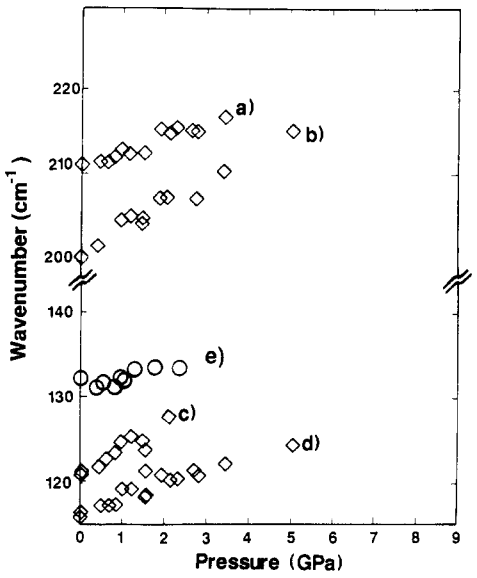

Figure 2. Pressure shift of the frequency of the (a) bulk Pt–Br stretch, (b) unassigned mode, (c) bulk Pt^{III}–Pt^{III} stretch, (d) bulk Pt^{II}–Pt^{II} stretch, and (e) defect Pt^{III}–Pt^{III} (O) stretch in DV–Pt_2Br (◇).

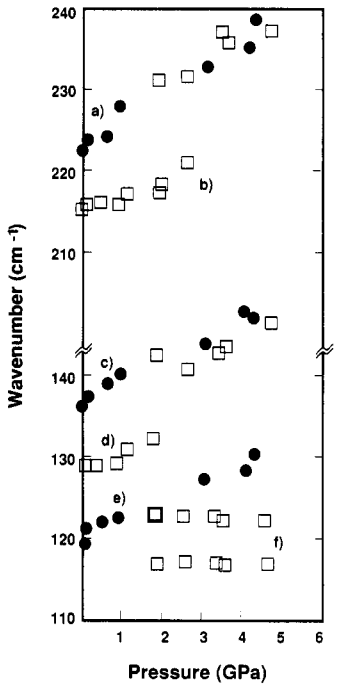

Figure 3. Pressure shift of the frequency of the (a) TV–Pt_2Br (●) Pt–Br stretch, (b) Pt_2Br_2 (□) Pt–Br stretch, (c) TV–Pt_2Br Pt^{III}–Pt^{III} stretch, (d) Pt_2Br_2 Pt^{III}–Pt^{III} stretch, (e) TV–Pt_2Br Pt^{II}–Pt^{II} stretch, and (f) converted Pt_2Br_2 Pt^{II}–Pt^{II} stretch.

TV–Pt_2Br to DV–Pt_2Br. Because of this conversion it was difficult to obtain good data on the complex.

The Raman spectra of DV–Pt_2Br at 40 K obtained at several pressures by using 676.4-nm excitation are published elsewhere.[22] As pressure was increased, the Pt–Br stretch (211 cm^{-1}) and the higher wavenumber Pt–Pt stretch (121 cm^{-1}) lost intensity and above ca. 4.0 GPa were no longer observed. The relative intensity of the 134- and 201-cm^{-1} features increased with increasing pressure. Pressure effects were reversible. Pressure-induced wavenumber shifts of modes observed in DV–Pt_2Br and TV–Pt_2Br are shown in Figures 2 and 3, respectively.

The 75 K Raman spectra of the bulk form of Pt_2Cl obtained in resonance with the IVCT band by using 568.2- and 514.5-nm excitation is shown in Figure 4. Raman

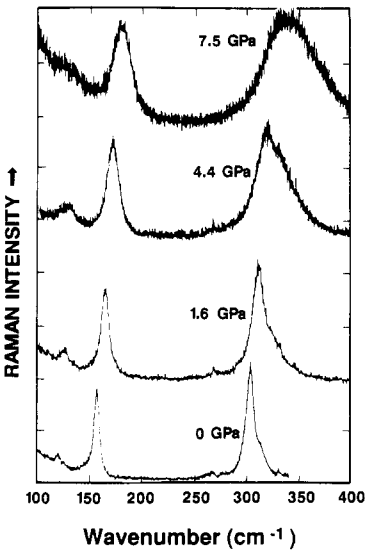

Figure 4. Raman spectra of bulk Pt_2Cl at several pressures by using 514.5-nm excitation.

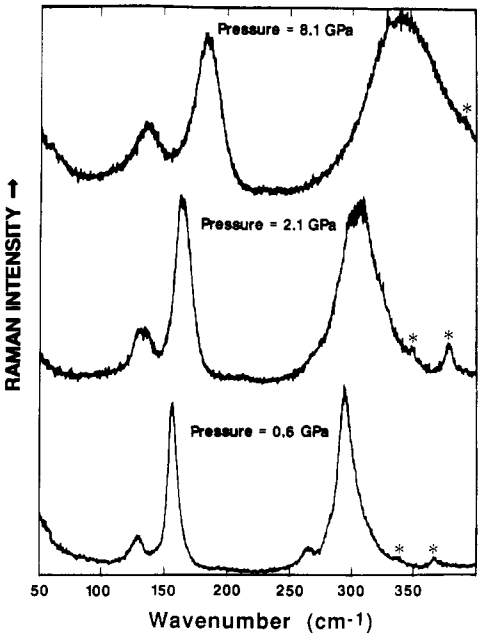

Figure 5. Raman spectra of the polaron state in Pt_2Cl at several pressures by using 676.4-nm excitation. The asterisked peaks are the ruby fluorescence.

spectra of the polaronic defect state in Pt_2Cl at 75 K were obtained by using 676.4-nm excitation (Figure 5). Details of the sample dependence of the polaron state are published elsewhere.[9] The relative intensity of the Pt^{II}–Pt^{II} stretch (125 cm^{-1}) attributed to the polaronic defect and the weak shoulder of the Pt–Cl stretch of the defect increased with increasing pressure. Similar effects were observed for the bulk; however, the increase in relative intensity of the Pt^{II}–Pt^{II} stretch (119 cm^{-1}) was much less. Considerable increase in the line widths of modes in both states was observed at higher pressures. All modes shifted to higher wavenumber with increasing pressure (Figure 6).[29] Pressure-induced wavenumber and line-width changes were reversible. In the spectra of the polaronic defect, five harmonic overtones of the Pt–X stretch were observed at 8.5 GPa.

(29) The high-frequency shoulder of the Pt–Cl stretch may have erroneously enhanced the shift of the Pt–Cl stretch. This is particularly true for the polaron state.

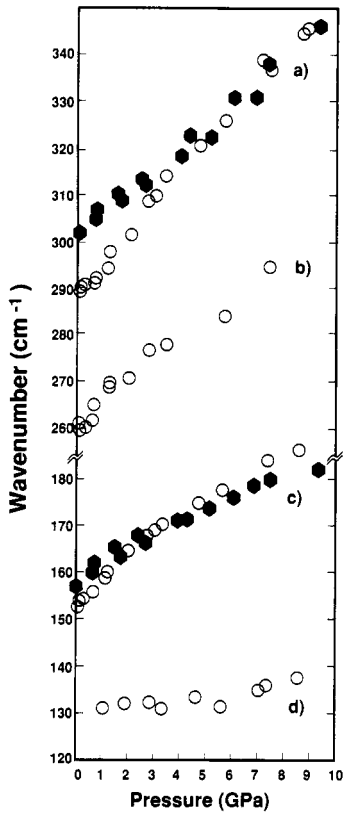

Figure 6. Pressure shift of the frequency of the (a) Pt–Cl stretch, (b) ring-bending mode, (c) Pt^{III}–Pt^{III} stretch, and (d) Pt^{II}–Pt^{II} stretch in the bulk (●) and polaron (○) states of Pt_2Cl.

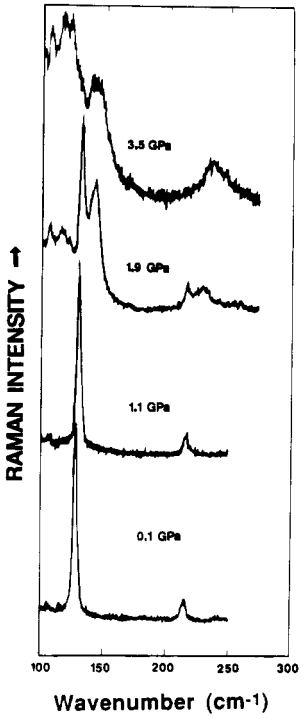

Figure 7. Raman spectra of Pt_2Br_2 at several pressures by using 514.5-nm excitation.

Pt_2X_2. Raman spectra of Pt_2Br_2 obtained at several pressures by using 514.5-nm excitation are shown in Figure 7. Below 1.7 GPa, the Pt^{III}–Pt^{III} (129 cm^{-1}) and the Pt–Br (216 cm^{-1}) stretching modes shift slightly to higher wavenumber with increasing pressure with little change in scattering intensity. Above 2.0 GPa the Pt–Br and the Pt^{III}–Pt^{III} modes of the starting complex lose intensity, and features are observed to grow in at 116, 123, 141, and 231 cm^{-1}.[30] Overall scattering intensity was also reduced considerably above 2.0 GPa. This disruptive change appeared to be reversible, with substantial increase in the line widths, if the sample was not pressurized beyond ca. 3.5 GPa. However, samples taken to higher pressures exhibited irreversible changes in the Raman spectra. Pressure-induced shifts of the modes observed in Pt_2Br_2 are shown in Figure 3.

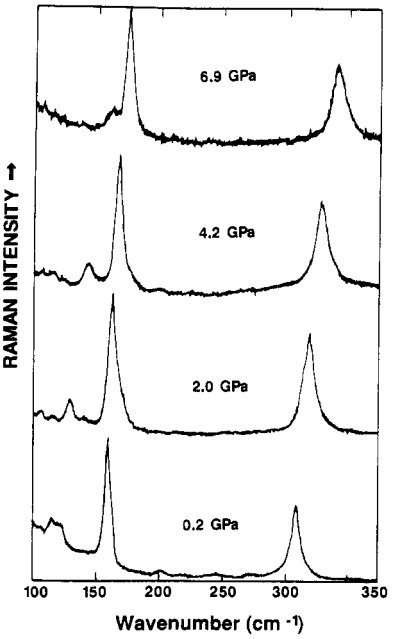

Figure 8. Raman spectra of Pt_2Cl_2 at several pressures by using 514.5-nm excitation.

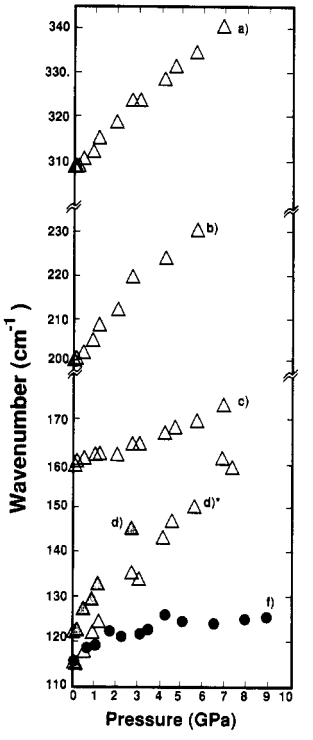

Figure 9. Pressure shift of the frequency of the (a) bulk Pt–Cl stretch, (b) unassigned mode, (c) bulk Pt^{III}–Pt^{III}, (d) defect Pt^{II}–Pt^{II} stretches in Pt_2Cl_2 (△), and (f) Pt^{II}–Pt^{II} stretch in Pt_2 (●).

The Raman spectra of Pt_2Cl_2 at 300 K were obtained at several pressures by using 514.5-nm excitation (Figure 8). Pressure-induced shifts of the modes are shown in

(30) The 141-cm^{-1} band may be two bands.

Figure 9. The 121-cm^{-1} band lost considerable intensity with increasing pressure and was no longer observed above 2.0 GPa. Some increase in intensity was observed initially for the 116-cm^{-1} mode. The 116- and 121-cm^{-1} modes exhibited unusually strong wavenumber shifts with increasing pressure. Above 7.5 GPa, scattering intensity was reduced considerably, and good data were not obtainable. On release to atmospheric pressure, changes in wavenumbers were reversible; however, considerable broadening of features occurred.

Pt_2. The pressure-induced wavenumber shift of the Pt^{II}–Pt^{II} (116 cm^{-1}) stretching mode in Pt_2 was obtained at room temperature by using 406.7- and 363.8-nm excitation (Figure 9). An initial blue shift with leveling at higher pressures was observed.

Discussion

Changes in the Raman spectra of these binuclear platinum diphosphite solids provide information about both the ground-state structures and defect states. This class of materials exhibits rich pressure dependence ranging from the expected changes in vibrational spectra (frequency shifts and line-shape changes) to structural phase changes indicative of enhanced valence delocalization as well as pressure-induced chemistry. The pressure-induced changes in the ground-state structures will be discussed first followed by a discussion of the behavior of defect states.

Pt_2X. Resonance Raman spectra of Pt_2X complexes obtained by exciting into the IVCT band are highly polarized along the chain axis, and the wavenumbers and intensities of the resonance-enhanced Raman modes have been used as a measure of the extent of valence delocalization.[3,13] Increased valence delocalization is expected to result in a lower wavenumber for the Pt^{III}–Pt^{III} and the Pt–X stretch and a higher wavenumber for the Pt^{II}–Pt^{II} stretch as electron density shifts out of the $d\sigma^*$ orbital of the Pt^{II}–Pt^{II} dimer and into of the $d\sigma^*$ orbital of the Pt^{III}–Pt^{III} dimer. In addition, the intensity of the Pt–X stretch relative to the Pt–Pt stretching modes for Pt_2X solids is directly related to the displacement of the halide off the center position. In the limit of going to a totally symmetric chain, the factor group is half the size of the original $P4/mbm$ cell and the Pt–X and the out-of-phase Pt–Pt stretching modes become Raman inactive.

Two forms of Pt_2Br exhibiting large differences in valence delocalization, TV–Pt_2Br and DV–Pt_2Br, have been identified on the basis of their Raman spectra by using the criteria discussed above. The ambient pressure wavenumbers for the Raman modes observed in TV–Pt_2Br and DV–Pt_2Br are consistent with the expected trends (Table I). In addition, the Pt–X stretch for the trapped-valence Pt_2Cl and Pt_2Br is quite strong, whereas the Pt–Br stretch in DV–Pt_2Br is weak.

TV–Pt_2Br and DV–Pt_2Br exhibit very different behavior at elevated pressure. In DV–Pt_2Br, decreases in the intensity of the Pt–X and one of the Pt–Pt stretching modes as pressure is increased are consistent with a continuous structural change toward a symmetric structure where the halide ions are located equidistant between the neighboring Pt_2 dimers. These intensity decreases are not observed in Pt_2Cl, indicating that this complex remains highly trapped valence until at least 10.0 GPa. TV–Pt_2Br exhibits some change in the relative intensities of these modes. However, on the basis of the wavenumber positions and intensities, this form of Pt_2Br remains largely trapped valence to 5.0 GPa.

Pressure-induced wavenumber shifts of Raman modes in Pt_2X solids also give insight into the differences in high-pressure behavior of Pt_2Cl and Pt_2Br. The wavenumbers of vibrational modes generally increase (blue shift) with increasing pressure due to an increase in the effective force constants with decreasing internuclear spacing. For the Pt_2X complexes increased delocalization is expected to reduce the magnitude of the blue shift of the Pt–X and the Pt^{III}–Pt^{III} stretches for the oxidized units while enhancing the blue shift for the Pt^{II}–Pt^{II} stretch for the reduced unit. (A detailed explanation of the pressure-induced shift of the Pt–X stretch in MX complexes has been published.)[19] Increased vibrational coupling, which results in an increase of the splitting of the wavenumber difference between the two modes involved, is also expected with increasing pressure and increased delocalization.

The magnitude of the blue shift of the wavenumber of the Pt–Cl stretch was somewhat weaker in Pt_2Cl than that observed in Pt_2Cl_2. In contrast, the blue shift of the Pt^{III}–Pt^{III} stretch was larger in Pt_2Cl than that observed in Pt_2Cl_2. These shifts are qualitatively consistent with increased valence delocalization and increased Pt^{III}–Pt^{III} and Pt^{II}–Pt^{II} coupling in Pt_2Cl with increasing pressure. The relative intensity increase of the Pt^{II}–Pt^{II} band may also reflect increased coupling with the Pt^{III}–Pt^{III} mode. Pressure-induced shifts of the IVCT band in the electronic spectra of Pt_2Cl also indicate that Pt_2Cl becomes more delocalized with increasing pressure.[21] Greater increase of the vibrational coupling between the Pt^{III}–Pt^{III} and Pt–X stretch in Pt_2Cl_2 than in Pt_2Cl with increasing pressure would also explain the observed shifts.

In the limited range in which data are available, the magnitude of the shift of the Pt–X stretch in DV–Pt_2Br is considerably less than that of the Pt–X stretch in TV–Pt_2Br. This observation is consistent with greater pressure-induced delocalization of DV–Pt_2Br relative to TV–Pt_2Br. The magntidue of the shifts of the Pt^{III}–Pt^{III} and Pt^{II}–Pt^{II} modes in both forms of Pt_2Br is similar. The effects of increased vibrational coupling between the Pt^{III}–Pt^{III} and Pt^{II}–Pt^{II} modes may be balancing the shifts resulting from changes in the charge on the Pt dimers with increased delocalization.

The Pt^{II}–Pt^{II} stretches in all of the Pt_2X complexes studied exhibit small shifts with increasing pressure, which may result from enhanced coupling with the higher lying Pt^{III}–Pt^{III} mode. However, the Pt^{II}–Pt^{II} stretch in Pt_2 (the $[(Bu)_4N]$ complex) also exhibits a weak shift with considerable leveling at high pressures.

An unusual feature of the high-pressure spectra of the bulk and polaron states in Pt_2Cl is the growth of intensity of a shoulder on the high-wavenumber side of the Pt–X stretch. This shoulder may be the first overtone of the Pt^{III}–Pt^{III} stretch, and the intensity increase may result from enhanced Fermi resonance between this overtone and the Pt–Cl stretch as the wavenumber separation between the two modes decreases with increasing pressure.

The Raman modes of the ground and polaron states in Pt_2Cl exhibit substantial line broadening with increasing pressure. This may have resulted from nonhydrostatic pressure conditions, increased structural inhomogeneities, or increased rates of vibrational dephasing at high pressure.[31]

Pt_2X_2. The Raman spectra of Pt_2Br_2 show a sharp discontinuity at ca. 2.0 GPa. The large difference in the observed frequencies and line widths of the new features that grow in above 2.0 GPa, relative to those of the low-pressure features, and the relatively poorer scattering cross

(31) (a) Gradients of 0.4 GPa were observed at high pressure. (b) The H_2O and K^+ ion positions are known to be disordered in Pt_2Cl.

sections at high pressure are indicative of a disruptive first-order phase transformation or a pressure-induced chemical change.

The frequencies of the two new modes observed at 116 and 121 cm^{-1} at high pressure are in reasonable agreement with the Pt^{II}–Pt^{II} stretch observed for the fully reduced complex $K_4[Pt_2(P_2O_5H_2)_4]\cdot 2H_2O$. On the basis of their frequencies and the weak shift of the energy of these bands with increasing pressure, the 116- and 121-cm^{-1} bands are tentatively attributed to Pt–Pt stretches for a reduced, Pt^{II}–Pt^{II}, fragment. The observation of two distinct frequencies for the Pt^{II}–Pt^{II} stretch may result from different orientations of the Pt_2 fragment within the lattice. In the electronic spectra, the appearance of a strong electronic absorption at 25 000 cm^{-1} above 2.0 GPa, which may by the $d\sigma^* \rightarrow p\sigma$ of the Pt_2 fragment, supports this assignment.[32]

The new Raman features at 141 and 231 cm^{-1} are substantially higher in frequency ($\sim$10 cm^{-1}) than the Pt^{III}–Pt^{III} and Pt–Br stretches, respectively, observed in the complex at low pressure. A possible explanation for the sharp disccontinuity observed in the spectra of Pt_2Br_2 at 2.0 GPa is that it is being disproportionated to Pt^{II}–Pt^{II} and Br–Pt^{IV}–Pt^{IV}–Br. The new Raman features at 141 and 231 cm^{-1} may then correspond to the Pt–Pt and Pt–Br stretches of a Br–Pt^{IV}–Pt^{IV}–Br fragment as would be consistent with pressure-induced disproportionations. Similar disproportionation was observed in $[Ni^{III}Cl_2(en)_2]Cl$, which disproportionated to a Ni^{II} and Ni^{IV} complex by moisture and pressure.[33]

However, the wavenumbers and pressure dependence of the new features at 141 and 231 cm^{-1} are very similar to those observed for the Pt^{III}–Pt^{III} and the Pt–Br stretches of TV–Pt_2Br (Figure 5). This similarity suggests that the Pt_2Br_2 fragment of the high-pressure complex may still be in the Pt^{III}–Pt^{III} oxidation state despite the substantial increase in the wavenumber of the Pt–Br and Pt–Pt stretches. In addition, the intensity of the Pt–Br stretch relative to the Pt^{III}–Pt^{III} in the low-pressure structure is small. In contrast in the high-pressure form, as well as in TV–Pt_2Br, the relative intensities are very similar. Accordingly, an alternative explanation for the discontinuity at 2.0 GPa is the decomposition of alternating Br–Pt^{IV}–Pt^{IV}–Br units to form Br_2 (in channels between the chains) and the reduced fragment, Pt^{II}–Pt^{II}. At present, we cannot distinguish between this model and disproportionation.

While Pt_2Br_2 undergoes a disruptive structural and possibly chemical change at modest pressures, Pt_2Cl_2 does not show evidence for any structural change when pressurized to 7.5 GPa. However, the loss of scattering intensity above 7.5 GPa and the significant line broadening observed on release from pressures well above 8.0 GPa suggest that a transformation may occur at high pressures in Pt_2Cl_2. The differences in the behavior of Pt_2Br_2 and Pt_2Cl_2 under pressure may result from the large differences in their crystal structures.[25]

Defects. The resonance Raman spectra of vibrational modes associated with defect states are strongly polarized along the chain axis. The effects of pressure on the Raman wavenumbers of these defect modes give insight into the changes in the extent of delocalization of the defect throughout the bulk with increasing pressure. It is expected that if a defect becomes more delocalized throughout the bulk at elevated pressures, the wavenumbers of the defect modes should approach those of the analogous bulk state modes.

In Pt_2Cl_2, weak modes at 116 and 121 cm^{-1} show excitation profiles and sample-dependent intensity variations that suggest that they may be the Pt^{II}–Pt^{II} stretch of reduced units of Pt_2 defect. As pressure is increased, the intensity of the 121-cm^{-1} feature irreversibly decreases rapidly while that of the 116-cm^{-1} feature increases. The 121-cm^{-1} defect mode is tentatively attributed to a metastable structural arrangement of the Pt_2 defect that rearranges at elevated pressure to that which gives rise to the 116-cm^{-1} feature. Both features shift to higher wavenumber and rapidly approach the wavenumber of the Pt^{III}–Pt^{III} stretch of the bulk with increasing pressure. This strong pressure dependence is attributed to increased delocalization of the defect charge density at elevated pressure. In effect, electron density is removed from the $d\sigma^*$ orbital of the Pt^{II}–Pt^{II} defect and distributed to neighboring Pt^{III}–Pt^{III} units as the charge on the Pt atoms of the defects approach that of the bulk lattice.

The wavenumbers of the modes for the polaron in Pt_2Cl also approach those of the analogous ground-state modes at elevated pressures (Figure 6). The shifts are consistent with increased delocalization of the defect as the bulk removes electron density from the $d\sigma^*$ orbital of the Pt^{III}–Pt^{III} dimer of the polaron and adds electron density to the $d\sigma^*$ orbital of the Pt^{II}–Pt^{II} dimer of the polaron. The long overtone progression of the Pt–X mode, observed in the Raman spectra of the polaron at 8.5 GPa, is consistent with the halogen being significantly displaced from the central position.[13] Though the defect appears to become more delocalized throughout the bulk with increasing pressure, it is still in a trapped valence state at high pressures.

In DV–Pt_2Br, the defect modes are consistent with short correlation segments of TV–Pt_2Br.[34] The evidence supporting these assignments are that the intensity of the modes shows strong excitation dependence that tracks that of TV–Pt_2Br, the intensity of these feature relative to the modes at 116, 121, and 212 cm^{-1} varies from sample to sample, and the wavenumbers of the modes are in agreement with that observed for the Pt^{III}–Pt^{III} and Pt–Br stretch in TV–Pt_2Br. In addition, at a given wavelength of laser light, the wavenumber of the defect modes vary by up to 6 cm^{-1} from sample to sample. This dispersion suggests that the segments of TV–Pt_2Br are perturbed by their surroundings, giving rise to inhomogeneous broadening of the defect electronic transition. The wavenumber of the Pt^{III}–Pt^{III} stretching mode of TV–Pt_2Br in DV–Pt_2Br exhibited little shift with increasing pressure (Figure 2). The expected blue shift with increasing pressure may be balanced by a weakening of the Pt^{III}–Pt^{III} bond of the defect as the defect becomes more delocalized.

Acknowledgment. We thank Dr. A. P. Sattleberger and Dr. M. H. Zietlow for synthesizing the complexes used in this study. We also thank Dr. H. G. Drickamer, Dr. S. D. Conradson, and Dr. S. F. Agnew for helpful discussions and technical assistance. This work was performed under the auspices of the U.S. Department of Energy with support from the Office of Basic Energy Sciences, Materials Science Division.

Registry No. Pt_2Cl, 99632-89-0; Pt_2Br, 85553-24-8; Pt_2Cl_2, 82135-56-6; Pt_2Br_2, 99632-91-4; Pt_2, 80011-26-3.

(32) At ambient pressure, $Pt_2(P_2O_5H_2)^{4-}$ has an intense absorption at 27 200 cm^{-1} which corresponds to the $d\sigma^* \rightarrow p\sigma$ transition.
(33) Yamashita, M.; Murase, I. *Inorg. Chim. Acta* **1985**, *97*, L43.
(34) It has not been possible to synthesize a Pt_2Br sample that is completely free of the defect.